

Nucleon structure from a light-front hamiltonian

S. Xu^{a,b*}, C. Mondal^{a,b}, Y. Li^{c,d}, X. Zhao^{a,b}, and J. P. Vary^c (BLFQ Collaboration)

^a*Institute of Modern Physics, Chinese Academy of Science, Lanzhou 730000, China.*

^b*School of Nuclear Science and Technology, University of Chinese Academy of Sciences, Beijing 100049, China.*

^c*Department of Physics and Astronomy, Iowa State University, Ames, Iowa 50011, USA.*

^d*Department of Modern Physics, University of Science and Technology of China, Hefei 230026, China.*

Received 19 January 2022; accepted 4 April 2022

We obtain the light-front wave functions (LFWFs) of the nucleon in the leading Fock sector representation using basis light-front quantization (BLFQ) approach. We adopt a light-front effective Hamiltonian, which includes a three-dimensional confining potential and a one-gluon exchange interaction with fixed coupling, and solve for its mass eigenstates. We then employ the LFWFs to compute the axial form factor and the transverse charge and magnetization densities for the nucleon. The axial form factor is found to be consistent with the experimental data. The charge and magnetization densities agree qualitatively with the phenomenological fits.

Keywords: Nucleon; light-front quantization; axial form factors; transverse densities.

DOI: <https://doi.org/10.31349/SuplRevMexFis.3.0308111>

1. Introduction

BLFQ [1] is a nonperturbative framework, which has emerged as a promising tool for solving relativistic bound-state problems in quantum field theories [2–10]. This approach is based on the Hamiltonian formalism and has been successfully applied to QED [2, 3, 11, 12] and QCD [4–10, 13–17] systems. In this work, we adopt a light-front effective Hamiltonian, which incorporates the light-front holographic QCD confinement potential [18] supplemented by a longitudinal confinement [4] along with the one-gluon exchange interaction with a fixed coupling constant. The LFWFs are obtained by diagonalizing the effective Hamiltonian and employed to calculate the axial form factors and the transverse charge and magnetization densities.

For the nucleon, the matrix element of the electromagnetic current is parameterized by two independent form factors (FFs), namely, the Dirac and the Pauli FFs. There are numerous dedicated experimental and theoretical efforts for studying the nucleon FFs [19–23]. The transverse charge and magnetization densities are defined through the two-dimensional Fourier transformation of the Dirac and Pauli FFs [24–28].

Unlike electromagnetic FFs, our information about the axial FFs is very narrow. Till date, there are only two sets of experiments, which determine the axial FFs, the charged pion electroproduction and the (anti)neutrino scattering off protons or nuclei [29, 30]. Meanwhile, the axial FFs have been investigated using various theoretical approaches [31–48]. Recently, the lattice QCD simulations of nucleon axial FF in 2 + 1 flavor near the physical pion mass has been reported by the PACS Collaboration [49].

2. Light-front hamiltonian

For the valence Fock sector of the nucleon, we adopt the following light-front effective Hamiltonian [9, 13]

$$H_{\text{eff}} = \sum_i \frac{m_i^2 + \vec{p}_{i\perp}^2}{x_i} + \frac{1}{2} \sum_{i,j} V_{i,j}^{\text{conf}} + \frac{1}{2} \sum_{i,j} V_{i,j}^{\text{OGE}}, \quad (1)$$

where m is the constituent mass of quark, $\sum_i x_i = 1$, and i, j indicate the index of particles in a Fock sector. $V_{i,j}^{\text{conf}}$ corresponds to the confining potential that includes both the longitudinal and the transverse confinements. The complete confining potential is given by

$$V_{i,j}^{\text{conf}} = \kappa^4 \vec{r}_{ij\perp}^2 + \frac{\kappa^4}{(m_i + m_j)^2} \partial_{x_i} (x_i x_j \partial_{x_j}), \quad (2)$$

where κ is the strength of the confining potential in both the longitudinal and transverse direction, $\vec{r}_{ij\perp} = \sqrt{x_i x_j} (\vec{r}_{i\perp} - \vec{r}_{j\perp})$ is the relative coordinate, and $\partial_x \equiv (\partial/\partial x)_{r_{ij\perp}}$. The third term in Eq. (1) corresponds to the one-gluon exchange (OGE) interaction:

$$V_{i,j}^{\text{OGE}} = \frac{4\pi C_F \alpha_s}{Q_{ij}^2} \bar{u}_{s'_i}(p'_i) \gamma^\mu u_{s_i}(p_i) \bar{u}_{s'_j}(p'_j) \gamma_\mu u_{s_j}(p_j), \quad (3)$$

with fixed coupling constant α_s , where $Q_{ij}^2 = -(1/2)(p'_i - p_i)^2 - (1/2)(p_j - p'_j)^2$ is the average of four-momentum square carried by the exchanged gluon and the color factor $C_F = -2/3$. The spinor $u_{s_i}(p_i)$ represents the solution of the free Dirac equation, with the subscripts denoting the spin and $\vec{p}_{i\perp}$ is the momentum of the quark i . We generate the dynamical spin structure in the LFWFs by implementing the OGE interaction.

For each Fock-particle we employ a two-dimensional harmonic-oscillator (2D-HO) wave function, $\phi_{n_i, m_i}(\vec{p}_{i\perp}; b)$

with b being the HO scale parameter, to describe its transverse degrees of freedom and a plane-wave to describe its longitudinal motion [2]. Diagonalizing the light-front Hamiltonian H_{eff} within the BLFQ basis, we obtain the eigenvalues that correspond to the mass spectrum. We also obtain the corresponding eigenvectors that represent the LFWFs in the BLFQ basis. The lowest eigenstate is naturally recognized as the nucleon state, labeled as $|P, \Lambda\rangle$, where the Λ denotes the helicity of the nucleon. The LFWFs in momentum space is then written as an expansion in the orthonormal basis [13]

$$\begin{aligned} \Psi_{\{x_i, \vec{p}_{i\perp}, \lambda_i\}}^\Lambda &= \langle P, \Lambda | \{x_i, \vec{p}_{i\perp}, \lambda_i\} \rangle \\ &= \sum_{\{n_i, m_i\}} (\psi_{\{x_i, n_i, m_i, \lambda_i\}}^\Lambda \prod_i \phi_{n_i, m_i}(\vec{p}_{i\perp}; b)), \end{aligned} \quad (4)$$

where $\psi_{\{x_i, n_i, m_i, \lambda_i\}}^\Lambda$ represents the LFWFs in BLFQ. We fix the model parameters by fitting the nucleon mass and the flavor FFs [13].

3. Results and discussions

Expanding the nucleon states with the BLFQ basis, the flavor Dirac and Pauli form factors can be expressed in terms of the

overlap of the nucleon LFWFs

$$\begin{aligned} F_1^q(Q^2) &= \sum_{\{\lambda_i\}} \int [d\mathcal{X} d\mathcal{P}_\perp] \Psi_{\{x'_i, \vec{p}'_{i\perp}, \lambda_i\}}^{\uparrow*} \Psi_{\{x_i, \vec{p}_{i\perp}, \lambda_i\}}^\uparrow; \quad (5) \\ F_2^q(Q^2) &= -\frac{2M}{(q^1 - iq^2)} \sum_{\{\lambda_i\}} \int [d\mathcal{X} d\mathcal{P}_\perp] \\ &\quad \times \Psi_{\{x'_i, \vec{p}'_{i\perp}, \lambda_i\}}^{\uparrow*} \Psi_{\{x_i, \vec{p}_{i\perp}, \lambda_i\}}^\downarrow, \end{aligned} \quad (6)$$

where $x'_1 = x_1$ and $\vec{p}'_{1\perp} = \vec{p}_{1\perp} + (1 - x_1)\vec{q}_\perp$ for the struck quark, whereas $x'_i = x_i$ and $\vec{p}'_{i\perp} = \vec{p}_{i\perp} - x_i\vec{q}_\perp$ for the spectators ($i = 2, 3$). Considering the frame, where $q^+ = 0$, $Q^2 = -q^2 = \vec{q}_\perp^2$. Here, we use the abbreviation

$$\begin{aligned} [d\mathcal{X} d\mathcal{P}_\perp] &= \prod_{i=1}^3 \left[\frac{dx_i d^2\vec{p}_{i\perp}}{16\pi^3} \right] \\ &\quad \times 16\pi^3 \delta\left(1 - \sum_{i=1}^3 x_i\right) \delta^2\left(\sum_{i=1}^3 \vec{p}_{i\perp}\right). \end{aligned} \quad (7)$$

Meanwhile, the nucleon FFs can be expressed using the flavor FFs as

$$F_{1(2)}^N = \sum_q e_q F_{1(2)}^q, \quad (8)$$

where N stands for the nucleon, and e_q is the quark charge.

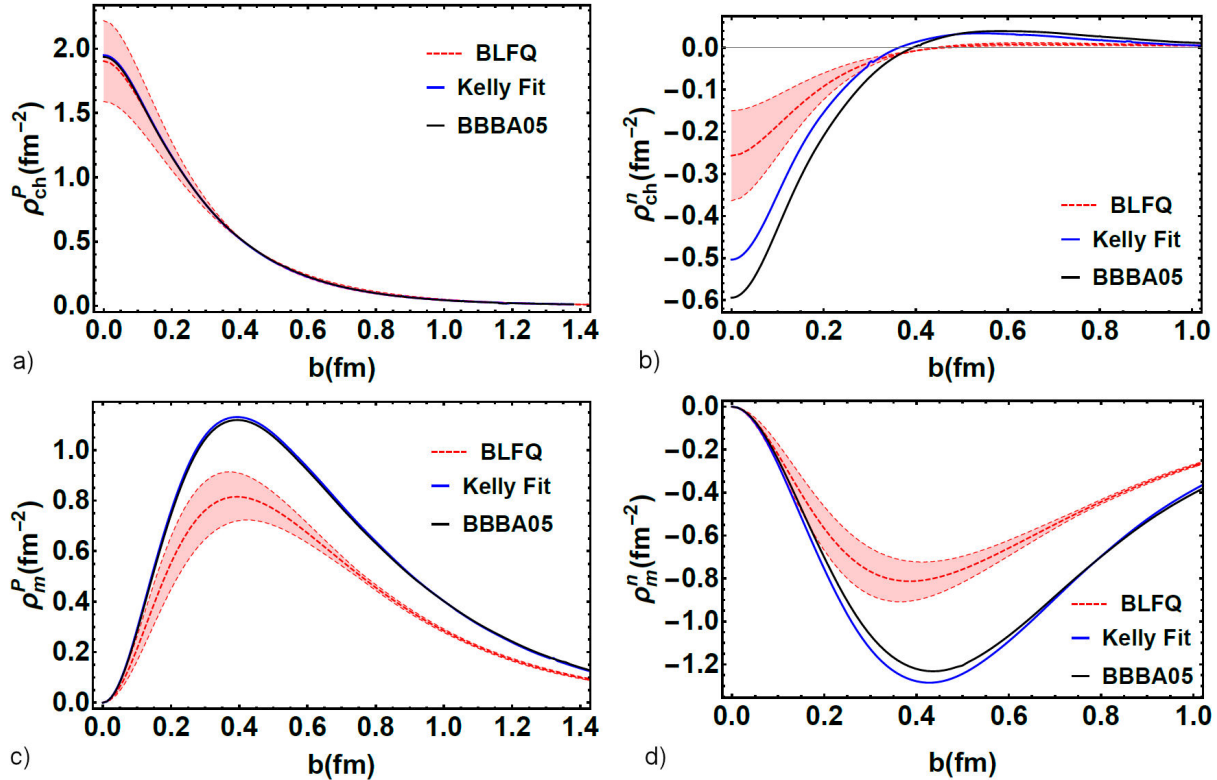


FIGURE 1. The transverse charge and anomalous magnetization densities for the unpolarized nucleon. a) and c) for the proton; b) and d) for the neutron. The red bands represent the uncertainty range of the BLFQ results. The blue and black lines correspond to the parameterizations of Kelly [50], and Bradford *et al.* [51], respectively.

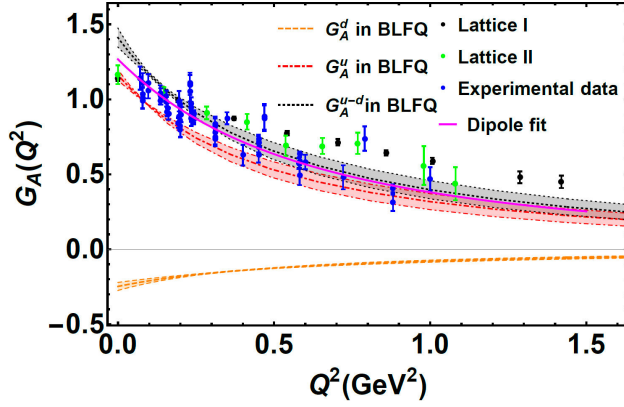


FIGURE 2. The axial form factors $G_A = G_A^u - G_A^d$ as the function of Q^2 . The gray band, red band, and orange band are the BLFQ results for G_A , G_A^u , and G_A^d , respectively. The blue circles represent the extracted data taken from the Refs. [29, 40] and the green and black circles correspond to the lattice calculations taken from [41]. The magenta line represents the dipole fit to the extracted data [29].

The transverse charge density of an unpolarized nucleon is written as the two-dimensional Fourier transform of the Dirac FF [24]

$$\rho_{\text{ch}}(b_{\perp}) = \int \frac{d^2 \vec{q}_{\perp}}{(2\pi)^2} F_1(Q^2) e^{i\vec{q}_{\perp} \cdot \vec{b}_{\perp}}, \quad (9)$$

where $b_{\perp} = |\vec{b}_{\perp}|$ defines the impact parameter. Similarly, the magnetization density is given by

$$\tilde{\rho}_{\text{m}}(b_{\perp}) = \int \frac{d^2 \vec{q}_{\perp}}{(2\pi)^2} F_2(Q^2) e^{i\vec{q}_{\perp} \cdot \vec{b}_{\perp}}, \quad (10)$$

while the anomalous magnetization density is defined as

$$\rho_{\text{fm}}(b_{\perp}) = -b_{\perp} \frac{\partial \tilde{\rho}_{\text{fm}}}{\partial b_{\perp}}. \quad (11)$$

We show the transverse densities of the nucleon in Fig. 1. We compare our results with the two different global parametrizations proposed by Kelly [50] and by Bradford *et al.* [51]. We observe that the proton charge density shows an excellent agreement with those global parameterizations. However, for the neutron transverse charge density, our current treatment predicts an insufficient magnitude. Although, the qualitative behavior of the neutron charge density agrees with the parametrizations. The behavior the anomalous magnetization densities for the nucleon in our model is also more or less in agreement with the global parametrizations, but our results are smaller in magnitude. Note that these results are computed within the leading Fock representation, while the higher Fock sectors $|qqqq\bar{q}\rangle$ and $|qqqg\rangle$ are anticipated to have significant effects on the Pauli FF and on the magnetization densities.

Based on our resulting LFWFs, the axial FF is given by

$$G_A^q(Q^2) = \sum_{\{\lambda_i\}} \int [d\mathcal{X} d\mathcal{P}_{\perp}] \times \lambda_1 \Psi_{\{x_i, \vec{p}_{i\perp}, \lambda_i\}}^{\uparrow*} \Psi_{\{x_i, \vec{p}_{i\perp}, \lambda_i\}}^{\uparrow}, \quad (12)$$

where $\lambda_1 = 1(-1)$ for the struck quark helicity.

We show our results for the axial FFs of the nucleon ($G_A = G_A^u - G_A^d$) and the contributions from the up and the down quark in $G_A(Q^2)$ in Fig. 2. We compare our results with the available extracted data from the (anti)neutrino scattering off protons or nuclei and charged pion electroproduction experiments [29, 30, 40] and the lattice QCD simulations from the Ref. [41]. Taking into consideration the experimental uncertainties, we find good consistency between our current treatment of the BLFQ computation and the experiment.

The axial FF is identified as the axial charge at $Q^2 = 0$. We obtain $g_A = 1.41 \pm 0.06$. The BLFQ result is somewhat larger than the extracted data 1.2723 ± 0.0023 [52]. The axial charge of the nucleon describes the difference of the spin carried by the up and the down quarks in the nucleon. In contrast with the extracted data, our prediction for the up quark is overestimated ($\Delta\Sigma_u \sim 1.1$), while the value of the down quark is underestimated ($\Delta\Sigma_d \sim 0.2$). Summing over the flavors, we find that the quark spin contributes $\sim 90\%$ to the proton spin in our current treatment for the nucleon, while the contribution of quark spin occupies only $\sim 40\%$ as reported from the experiment [53]. This evident discrepancy suggests the need to extend our model to incorporate the higher Fock components, which have a notable effect on the quark contribution to the nucleon spin.

4. Conclusions

We adopted an effective light-front Hamiltonian that incorporates confinement in both the transverse and the longitudinal direction and one gluon exchange interaction for the valence quarks suitable for low-resolution properties. We obtained the nucleon LFWFs by solving its mass eigenstates. We then employed the LFWFs to compute the nucleon axial FFs, and the transverse charge and magnetization densities.

We computed the transverse charge and magnetization densities by employing the two dimensional Fourier transformation of the Dirac and Pauli FFs. We found that the BLFQ results are qualitatively consistent with the global parameterizations.

We also evaluated the axial form factor of the nucleon from our resulting LFWFs. We found that the proton axial form factor is in a good agreement with the experimental data. However, the axial charge of the proton is somewhat overestimated as compared to the extracted data. We also noticed that the quark spin contribution to the proton spin is significantly larger (91%) than the expected result from the experiment (40%). This emerges due to the fact that our current treatment does not consider the higher Fock sectors. With

dynamical gluons and sea quarks, the quark spin contribution can be reduced and the orbital angular momentum can play a important role in understanding the nucleon spin.

Acknowledgment

C. M. is supported by new faculty start up funding by the Institute of Modern Physics, Chinese Academy of Sciences, Grant No. E129952YR0. C. M. also thanks the Chinese Academy of Sciences Presidents International Fellowship Initiative for the support via Grant No. 2021PM0023. X. Z. is supported by new faculty startup funding by the Institute of Modern Physics, Chinese Academy of Sciences,

by the Key Research Program of Frontier Sciences, Chinese Academy of Sciences, Grant No. ZDB-SLY-7020, by the Natural Science Foundation of Gansu Province, China, Grant No. 20JR10RA067, and by the Strategic Priority Research Program of the Chinese Academy of Sciences, Grant No. XDB34000000. J. P. V. is supported by the Department of Energy under Grants No. DE-FG02-87ER40371 and No. DE-SC0018223 (SciDAC4/NUCLEI). This research used resources of the National Energy Research Scientific Computing Center (NERSC), a U.S. Department of Energy Office of Science User Facility operated under Contract No. DE-AC02-05CH11231.

-
1. J. P. Vary *et al.* Hamiltonian light-front field theory in a basis function approach, *Phys. Rev. C* **81** (2010) 035205. <https://doi.org/10.1103/PhysRevC.81.035205>.
 2. X. Zhao, H. Honkanen, P. Maris, J. P. Vary and S. J. Brodsky, Electron $g-2$ in Light-Front Quantization, *Phys. Lett. B* **737** (2014) 65-69. <https://doi.org/10.1016/j.physletb.2014.08.020>.
 3. P. Wiecki, Y. Li, X. Zhao, P. Maris and J. P. Vary, Basis Light-Front Quantization Approach to Positronium, *Phys. Rev. D* **91** (2015) 105009. <https://doi.org/10.1103/PhysRevD.91.105009>.
 4. Y. Li, P. Maris, X. Zhao and J. P. Vary, Heavy Quarkonium in a Holographic Basis, *Phys. Lett. B* **758** (2016) 118-124. <https://doi.org/10.1016/j.physletb.2016.04.065>.
 5. S. Tang, Y. Li, P. Maris and J. P. Vary, B_c mesons and their properties on the light front, *Phys. Rev. D* **98** (2018) 114038. <https://doi.org/10.1103/PhysRevD.98.114038>.
 6. S. Jia and J. P. Vary, Basis light front quantization for the charged light mesons with color singlet Nambu–Jona-Lasinio interactions, *Phys. Rev. C* **99** (2019) 035206. <https://doi.org/10.1103/PhysRevC.99.035206>.
 7. J. Lan, C. Mondal, S. Jia, X. Zhao and J. P. Vary, Parton Distribution Functions from a Light Front Hamiltonian and QCD Evolution for Light Mesons, *Phys. Rev. Lett.* **122** (2019) 172001. <https://doi.org/10.1103/PhysRevLett.122.172001>.
 8. W. Qian, S. Jia, Y. Li and J. P. Vary, Light mesons within the basis light-front quantization framework, *Phys. Rev. C* **102** (2020) 055207. <https://doi.org/10.1103/PhysRevC.102.055207>.
 9. C. Mondal *et al.*, Proton structure from a light-front Hamiltonian, *Phys. Rev. D* **102** (2020) 016008. <https://doi.org/10.1103/PhysRevD.102.016008>.
 10. J. Lan *et al.*, Light mesons with one dynamical gluon on the light front, *Phys. Lett. B* **825** (2022) 136890. <https://doi.org/10.1016/j.physletb.2022.136890>.
 11. D. Chakrabarti, X. Zhao, H. Honkanen, R. Manohar, P. Maris and J. P. Vary, Generalized parton distributions in a light-front nonperturbative approach, *Phys. Rev. D* **89** (2014) 116004. <https://doi.org/10.1103/PhysRevD.89.116004>.
 12. Z. Hu, S. Xu, C. Mondal, X. Zhao, J. P. Vary [BLFQ], Transverse structure of electron in momentum space in basis light-front quantization, *Phys. Rev. D* **103** (2021) 036005. <https://doi.org/10.1103/PhysRevD.103.036005>.
 13. S. Xu, C. Mondal, J. Lan, X. Zhao, Y. Li, J. P. Vary [BLFQ], Nucleon structure from basis light-front quantization, *Phys. Rev. D* **104** (2021) 094036. <https://doi.org/10.1103/PhysRevD.104.094036>.
 14. L. Adhikari, C. Mondal, S. Nair, S. Jia, X. Zhao, J. P. Vary [BLFQ], Generalized parton distributions and spin structures of light mesons from a light-front Hamiltonian approach, *Phys. Rev. D* **104** (2021) 114019. <https://doi.org/10.1103/PhysRevD.104.114019>.
 15. C. Mondal S. Nair, S. Jia, X. Zhao, J. P. Vary [BLFQ], Pion to photon transition form factors with basis light-front quantization, *Phys. Rev. D* **104** (2021) 094034. <https://doi.org/10.1103/PhysRevD.104.094034>.
 16. J. Lan *et al.*, Parton Distribution Functions of Heavy Mesons on the Light Front, *Phys. Rev. D* **102** (2020) 014020. <https://doi.org/10.1103/PhysRevD.102.014020>.
 17. J. Lan, C. Mondal, S. Jia, X. Zhao and J. P. Vary, Pion and kaon parton distribution functions from basis light front quantization and QCD evolution, *Phys. Rev. D* **101** (2020) 034024. <https://doi.org/10.1103/PhysRevD.101.034024>.
 18. S. J. Brodsky, G. F. de Teramond, H. G. Dosch and J. Erlich, Light-Front Holographic QCD and Emerging Confinement, *Phys. Rept.* **584** (2015) 1-105. <https://doi.org/10.1016/j.physrep.2015.05.001>.
 19. H. Y. Gao, *Int. J. Mod. Phys. E* **12** (2003) 1.
 20. C. E. Hyde-Wright and K. de Jager, *Ann. Rev. Nucl. Part. Sci.* **54** (2004) 217.
 21. C. F. Perdrisat, V. Punjabi and M. Vanderhaeghen, *Prog. Part. Nucl. Phys.* **59** (2007) 694.
 22. S. Pacetti, R. Baldini Ferroli and E. Tomasi-Gustafsson, Proton electromagnetic FFs: Basic notions, present achievements and future perspectives, *Phys. Rept.* **550-551** (2015) 1.

23. V. Punjabi, C. F. Perdrisat, M. K. Jones, E. J. Brash and C. E. Carlson, The Structure of the Nucleon: Elastic Electromagnetic FFs, *Eur. Phys. J. A* **51** (2015) 79.
24. G. A. Miller, Charge Density of the Neutron, *Phys. Rev. Lett.* **99** (2007) 112001. <https://doi.org/10.1103/PhysRevLett.99.112001>.
25. C. E. Carlson and M. Vanderhaeghen, Empirical transverse charge densities in the nucleon and the nucleon-to-Delta transition, *Phys. Rev. Lett.* **100** (2008) 032004. <https://doi.org/10.1103/PhysRevLett.100.032004>.
26. D. Chakrabarti and C. Mondal Generalized parton distributions and transverse densities in a light-front quark-diquark model for the nucleons, *Eur. Phys. J. C* **74** (2014) 2962.
27. C. Mondal and D. Chakrabarti, Generalized parton distributions and transverse densities in a light-front quark-diquark model for the nucleons, *Eur. Phys. J. C* **75** (2015) 261. <https://doi.org/10.1140/epjc/s10052-015-3486-6>.
28. C. Mondal, Form factors and transverse charge and magnetization densities in the hard-wall AdS/QCD model, *Phys. Rev. D* **94** (2016) 073001. <https://doi.org/10.1103/PhysRevD.94.073001>.
29. V. Bernard, L. Elouadrhiri and U. G. Meissner, Axial structure of the nucleon: Topical Review, *J. Phys. G* **28** (2002) R1. <https://doi.org/10.1088/0954-3899/28/1/201>.
30. M. R. Schindler and S. Scherer, Nucleon Form Factors of the Isovector Axial-Vector Current: Situation of Experiments and Theory, *Eur. Phys. J. A* **32** (2007) 429. https://doi.org/10.1007/978-3-540-74413-9_10.
31. K. Tsuchida, T. Yamaguchi, Y. Kohyama and K. Kubodera, Weak Interaction Form-factors and Magnetic Moments of Octet Baryons: Chiral Bag Model With Gluonic Effects, *Nucl. Phys. A* **489** (1988) 557. [https://doi.org/10.1016/0375-9474\(88\)90111-X](https://doi.org/10.1016/0375-9474(88)90111-X).
32. B. Julia-Diaz, D. O. Riska and F. Coester, Axial transition form-factors and pion decay of baryon resonances, *Phys. Rev. C* **70** (2004) 045204. <https://doi.org/10.1103/PhysRevC.70.045204>.
33. S. Mamedov, B. B. Sirvanli, I. Atayev and N. Huseynova, Nucleon's axial-vector form factor in the hard-wall AdS/QCD model, *Int. J. Theor. Phys.* **56** (2017) 1861. <https://doi.org/10.1007/s10773-017-3330-x>.
34. X. Y. Liu, K. Khosonthongkee, A. Limphirat and Y. Yan, Comparisons of magnetic charge and axial charge meson cloud distributions in the PCQM, *Sci. Rep.* **7** (2017) 8139. <https://doi.org/10.1038/s41598-017-08648-w>.
35. I. V. Anikin, V. M. Braun and N. Offen, Axial form factor of the nucleon at large momentum transfers, *Phys. Rev. D* **94** (2016) 034011. <https://doi.org/10.1103/PhysRevD.94.034011>.
36. C. Adamuscin, E. Tomasi-Gustafsson, E. Santopinto and R. Bijker, Two-component model for the axial form factor of the nucleon, *Phys. Rev. C* **78** (2008) 035201. <https://doi.org/10.1103/PhysRevC.78.035201>.
37. I. G. Aznauryan *et al.*, Studies of Nucleon Resonance Structure in Exclusive Meson Electroproduction, *Int. J. Mod. Phys. E* **22** (2013) 1330015. <https://doi.org/10.1142/S0218301313300154>.
38. C. Mondal, Helicity-dependent generalized parton distributions for nonzero skewness, *Eur. Phys. J. C* **77** (2017) 640. <https://doi.org/10.1140/epjc/s10052-017-5203-0>.
39. G. Ramalho, Holographic estimate of the meson cloud contribution to nucleon axial form factor, *Phys. Rev. D* **97** (2018) 073002. <https://doi.org/10.1103/PhysRevD.97.073002>.
40. H. Hashamipour, M. Goharipour and S. S. Gousheh, Nucleon axial form factor from generalized parton distributions, *Phys. Rev. D* **100** (2019) 016001. <https://doi.org/10.1103/PhysRevD.100.016001>.
41. C. Alexandrou *et al.*, Nucleon form factors and moments of generalized parton distributions using $N_f = 2 + 1 + 1$ twisted mass fermions, *Phys. Rev. D* **88** (2013) 014509. <https://doi.org/10.1103/PhysRevD.88.014509>.
42. T. Bhattacharya, S. D. Cohen, R. Gupta, A. Joseph, H. W. Lin and B. Yoon, Nucleon Charges and Electromagnetic Form Factors from 2+1+1-Flavor Lattice QCD, *Phys. Rev. D* **89** (2014) 094502. <https://doi.org/10.1103/PhysRevD.89.094502>.
43. J. Liang, Y. B. Yang, K. F. Liu, A. Alexandru, T. Draper and R. S. Sufian, Lattice Calculation of Nucleon Isovector Axial Charge with Improved Currents, *Phys. Rev. D* **96** (2017) 034519. <https://doi.org/10.1103/PhysRevD.96.034519>.
44. J. Green *et al.*, Up, down, and strange nucleon axial form factors from lattice QCD, *Phys. Rev. D* **95** (2017) 114502. <https://doi.org/10.1103/PhysRevD.95.114502>.
45. D. L. Yao, L. Alvarez-Ruso and M. J. Vicente-Vacas, Extraction of nucleon axial charge and radius from lattice QCD results using baryon chiral perturbation theory, *Phys. Rev. D* **96** (2017) 116022. <https://doi.org/10.1103/PhysRevD.96.116022>.
46. A. Abdel-Rehim *et al.*, Nucleon and pion structure with lattice QCD simulations at physical value of the pion mass, *Phys. Rev. D* **92** (2015) 114513. <https://doi.org/10.1103/PhysRevD.92.114513>; Erratum: [*Phys. Rev. D* **93** (2016) 039904]. <https://doi.org/10.1103/PhysRevD.93.039904>.
47. G. S. Bali *et al.* Nucleon isovector couplings from $N_f = 2$ lattice QCD, *Phys. Rev. D* **91** (2015) 054501. <https://doi.org/10.1103/PhysRevD.91.054501>.
48. T. Bhattacharya, V. Cirigliano, S. Cohen, R. Gupta, H. W. Lin and B. Yoon, Axial, Scalar and Tensor Charges of the Nucleon from 2+1+1-flavor Lattice QCD, *Phys. Rev. D* **94** (2016) 054508. <https://doi.org/10.1103/PhysRevD.94.054508>.
49. K. I. Ishikawa *et al.*, *Phys. Rev. D* **98** (2018) 074510. <https://doi.org/10.1103/PhysRevD.98.074510>.
50. J. J. Kelly, Simple parametrization of nucleon form factors, *Phys. Rev. C* **70** (2004) 068202. <https://doi.org/10.1103/PhysRevC.70.068202>.

51. R. Bradford, A. Bodek, H. S. Budd and J. Arrington, A New parameterization of the nucleon elastic form-factors, *Nucl. Phys. B Proc. Suppl.* **159** (2006) 127-132. <https://doi.org/10.1016/j.nuclphysbps.2006.08.028>.
52. M. Tanabashi *et al.*, Review of Particle Physics, *Phys. Rev. D* **98** (2018) 030001. <https://doi.org/10.1103/PhysRevD.98.030001>.
53. E. Leader, A. V. Sidorov and D. B. Stamenov, Determination of Polarized PDFs from a QCD Analysis of Inclusive and Semi-inclusive Deep Inelastic Scattering Data, *Phys. Rev. D* **82** (2010) 114018. <https://doi.org/10.1103/PhysRevD.82.114018>.